Cancer Management and Research

Dovepress
open access to scientific and medical research

Open Access Full Text Article

ORIGINAL RESEARCH

Inhibition of human glioblastoma cell invasion involves PION@E6 mediated autophagy process

This article was published in the following Dove Medical Press journal:
Cancer Management and Research

Zhongyu Ren
Jing Liang
Peng Zhang
Jianjiao Chen
Jian Wen

Affiliated Hospital of Guilin Medical University, Guilin Medical University, Guangxi, People's Republic of China

Background: Glioblastoma (GBM) is the most severe brain cancer due to its ability to invade surrounding brain tissue. Iron oxide nanoparticles (ION) could effectively induce a decrease of cell migration/invasion. Also IONs could generate ROS stress which induces autophagy elevation. Autophagy is associated with both anti-tumorigenesis and protumorigenesis.
Objective: To explore the effect of PEGylated IONs (PION@E6) on the GBM cell invasion and its mechanism based on autophagy.
Materials and methods: PION@E6 were prepared and characterized according to our previous study. After incubation of U251 cells with PION@E6, cellular uptake of PION@E6 and cell viability were tested by Prussian blue staining and Cell Counting Kit-8, respectively. The migration and invasive capability was assessed by transwell cell migration and invasion assay. Expressions of autophagy biomarkers were detected by Western blotting. Intracellular ROS level was determined using 2′–7′-dichlorodihydrofluorescein diacetate.
Results: Average hydrate particle size and zeta potential of PION@E6 were 37.86±12.90 nm and –23.8 mV, respectively, and uniformly distributed nanoparticles with an average diameter of 10 nm were observed by TEM. Chlorin e6 successfully incorporated onto PION@E6 was demonstrated by ultraviolet and visible absorption spectrophotometry, and PION@E6 owning excellent water solubility and stability were showed by Colloid stability test. PION@E6 were successfully taken up by U251 cells with Prussian blue staining, and they showed in vitro cytotoxicity to glioma cells after long incubation of 72 hours. Migration/invasion of cells was significantly inhibited by PION@E6, which could be counteracted by pretreatment with 3-MA. Additionally, the expression of beclin-1, IC3I, and IC3II proteins was higher, whereas that of p62 protein was lower. Moreover, a dose dependent intracellular ROS generation of PION@E6 was detected.
Conclusion: Invasiveness of human GBM cells involves the PION@E6-mediated autophagy process, which may be related to the intracellular ROS induced by PION@E6.
Keywords: iron oxide nanoparticle, glioblastoma, invasiveness, autophagy

Introduction

Glioblastoma (GBM) is the most aggressive cancer that begins within the brain with the worst prognosis and survival time. Despite the great advances in therapeutic strategies, including surgery, chemotherapy and radiotherapy, the prognosis is still unfavorable and the recurrence rate is at about 98% with the median overall survival of 12–15 months,[1,2] owing to rapid emergence of tumor resistance and side effects of current chemotherapeutic agents. This poor outcome and high recurrence rate highlight the need to explore novel anti-GBM ways with fewer side-effects and greater therapeutic efficiency.

Correspondence: Jian Wen
Affiliated Hospital of Guilin Medical University, Guilin Medical University, Guangxi, 541040, People's Republic of China
Tel +86 189 9404 3727
Email wenjian2400@163.com

submit your manuscript | www.dovepress.com
Dovepress
http://dx.doi.org/10.2147/CMAR.S200151

The aggressiveness of this cancer is largely due to its ability to invade surrounding brain tissue, making the tumor difficult to remove by surgery. Thus, the invasiveness of tumor cells is among the major obstacles for GBM treatment and the principal cause of poor prognosis in patients with GBM, and many researchers are trying to find ways to inhibit the invasiveness of GBM.[3] In recent years, nanomedicine has become an attractive approach for targeted drug delivery and for new therapeutic strategies able to overcome the traditional limitations due to toxicity, healthy tissue damage, or other undesired side effects of direct drug administration.[4]

Iron oxide nanoparticles (IONs), a noncytotoxic reagent, could effectively induce a decrease of cell migration/invasion in K-ras transformed cells and endometrial cells, cytoskeleton and cell motility capacity were greatly affected after IONs incubation even at low iron concentration (0.1 mm).[5,6] In our previous study of PEGylated IONs (PION@E6), we demonstrated that IONs as nanocarriers to improve chlorin e6 (E6)-based sonosensitivity in impairment of cancer cells viability.[7] Thus, PION@E6 may be a potential noncytotoxic way to inhibit GBM invasion. Moreover, IONs could generate ROS which could induce autophagy for cytoprotection.[8]

Autophagy is a catabolic process in which eukaryotic cells remove abnormal proteins and damaged organelles through lysosomal degradation.[9] A previous study has indicated that autophagy is a novel approach to anticancer therapy.[10] Moreover, autophagy elevation has an antitumor function[11] and inhibits the invasion of breast cancer cells independent of oxygenation conditions.[12] However, some studies reported a protumorigenesis effect associated with autophagy elevation.[13]

To elucidate the effect of autophagy on the invasiveness of U251 cells (derived from a human GBM tumor) in the setting of IONs treatment, we explored the effect of PION@E6 on the invasiveness of U251 cells and its possible underlying mechanism via autophagy.

Materials and methods

Reagents and culture medium

Acetone, ethanol, ferrous chloride ($FeCl_2$), tris (acetylacetonato) iron (III) ($Fe(acac)_3$), oleic, oleic acid, oil amine, 1,2-distearoyl-sn-glycero-3-phosphoethanolamine-N-[amino (polyethylene glycol)–2000] (DSPE-PEG 2000), and E6 were purchased from Guoyao Chemical Inc. (Shanghai, China). DMEM and FBS were bought from Thermo Fisher Scientific (Waltham, MA, USA). Cell Counting Kit-8 (CCK-8) was obtained from Dojindo Laboratories (Kumamoto, Japan). And 2′–7′-dichlorodihydrofluorescein diacetate (DCFH-DA) was purchased from Sigma-Aldrich Co. (St Louis, MO, USA).

Synthesis of PION@E6

PION@E6 was prepared according to our previous study.[7] Briefly, IONs coated with oleic acid were first prepared by means of high temperature pyrolysis. Then, 50 mg DSPE-PEG 2000 and 10 mg E6 were added to the mixture of IONs coated with oleic acid to synthesize PION@E6 following the preparation protocol.[7]

Characterization of PION@E6

The particle sizes and zeta potential of PION@E6 were measured using a Brookhaven-zeta plus Particle Analysis Device (Brookhaven Instruments Corporation, NY, USA) and a Zeta Potential Device (Nanjing Fuxin Analysis, China), respectively. Morphological characteristics of PION@E6 were observed and photographed by Philips CM300 transmission electron microscopy (TEM) images. Analysis of ultraviolet-visible-near-infrared absorbance spectra and fluorescent spectra of free E6 and PION@E6 were carried out using a UV-2700 UV-VIS Spectrophotometer (Shimadzu, Kyoto, Japan) and an F-7000 Fluorescence Spectrophotometer (Hitachi Ltd., Tokyo, Japan), respectively. In addition, the stability of PION@E6 dissolved in deionized water was determined and further aggregation of PION@E6 was tested by colloid stability test after 5 weeks.

Principles of cell culture

Human glioblastoma cell line U251 was obtained from American Type Culture Collection (ATCC; Manassas, VA, USA). The cells were maintained and cultured in DMEM supplemented with 10% FBS, 100 U/mL penicillin and 100 μg/mL streptomycin in a humidified atmosphere of 5% CO_2 incubator at 37°C. The cultivating media was refreshed every 3 days, and U251 cells in the logarithmic growth phase were used to conduct the experiments described as follows.

Cellular iron uptake with Prussian blue staining assessment

To directly prove the intracellular particulate iron of PION@E6, U251 cells were incubated with PION@E6 for 2 hours and then washed twice with prewarmed PBS and dried at 37°C. With Prussian blue staining assessment, the intracellular particulate iron of PION@E6 was assessed according to the manufacturer's instruction (Beijing Solarbio Science & Technology Co., Ltd, Beijing, China).

Cell viability

According to the manufacture's instruction, CCK-8 assay was performed to measure the viability of U251 cells. Briefly, U251 cells were incubated with different concentration of PION@E6 (25, 50, 100, and 200 μg/mL) and those incubated without PION@E6 were used as negative controls for each analysis. After incubation for 24 hours, the cells were washed three times with 200 μL PBS/well to minimize the interference of PION@E6. Then, 10 μL CCK-8 solution was added to each well and incubated for an additional 4 hours, the optical density of each well at 450 nm was determined using a BioTek microplate reader (BioTek Instruments Inc., Winooski, VT, USA) .

Transwell cell migration and invasion assay

The assay was performed in a 24 well invasion plate based on the Boyden Chamber principle. Briefly, U251 cells were incubated with different concentrations of PION@E6 for 24 hours. Then the cells were harvested and seeded into the upper chamber in medium (100 μL) with 1% FBS.

Cell migration was observed by their movement from the upper chamber with serum-containing medium (1%) to the lower chamber with serum-containing medium (20%) through an 8 μm pore size transwell membrane. After incubation at 37°C with 5% CO_2 for 12 hours, migratory cells that have passed through membrane pores were fixed, stained, and counted by crystal violet staining according to the manufacturer's instruction.

Cell invasion assay was performed by adding extracellular matrix (ECM) materials on top of the transwell membrane and then adding cells on top of the ECM. Briefly, 30 μL of Matrigel (BD Biosciences, San Jose, CA, USA) was added to a 24-well transwell insert (Corning Incorporated, Corning, NY, USA) and solidified for 15–30 minutes to form a thin gel layer. Then cell invasion was observed by their movement from the upper chamber with serum-containing medium (1%) to the lower chamber with serum-containing medium (20%) through an 8 μm pore size transwell membrane coated with a thin layer of Matrigel ECM layer. After incubation at 37°C with 5% CO_2 for 24 hours, invading cells that have passed through membrane pores were fixed, stained, and counted by crystal violet staining according to the manufacturer's instruction.

Expression of IC3I, IC3II, beclin-1, p62 by Western blotting

After incubation with various concentrations of PIONs@E6 for 24 hours, U251 cells were homogenized in lysis buffer, separated by 10% SDS-PAGE, and transferred to PVDF membranes (IPVH00010, EMD Millipore, Billerica, MA, USA). Membranes were blocked with 5% skimmed milk and then incubated with diluted primary antibodies including rabbit anti-P62 (1:10000; ab109012, Abcam, MA, USA), anti-beclin-1(1:2000; ab207612, Abcam), anti-LC3II (1:2000; ab192890, Abcam), anti-LC3I (1:2000; ab192890, Abcam), and anti-GAPDH (1:1000; ab181602, Abcam). Blots were washed with TBS/TWEEN and incubated with an appropriate horseradish peroxidase-conjugated secondary antibody (1:5000; KGAA35, Keygen Inc., Nanjing, P.R.C) for 2 hours. After washing with TBS/TWEEN, the blots were developed with the chemiluminescence method (ECL Luminata Crescendo, WBLUR0500, EMD Millipore).

Measurement of intracellular ROS level

Intracellular ROS level of U251 cells was determined by DCFH-DA staining. Briefly, U251 cells were incubated with 0, 50, 100, and 200 μg/mL PION@E6 at 37°C and those incubated with 0 μg/mL PION@E6 were regarded as negative controls. After incubation for 12 hours, the cells were washed three times with PBS to minimize the interference and then incubated with 20 μM DCFH-DA for 30 minutes at 37°C. Thereafter, the cells were washed twice with PBS and monitored at an excitation wavelength of 485 nm and an emission wavelength of 535 nm using Spectra Max M2 fluorescence microplate reader (Molecular Devices LLC, Sunnyvale, CA, USA). Data were expressed as percentage fluorescence compared with relevant negative controls.

Statistical analysis

Data were presented as mean ± SD and analyzed with either Student's *t*-test or ANOVA using SPSS13.0 (SPSS Inc., Chicago, IL, USA). $P<0.05$ was considered statistically significant.

Results

Preparation and characterization of PION@E6

Oleic acid coated IONs was synthesized by means of high temperature pyrolysis using chemicals $FeCl_2$, oleic acid and $Fe(acac)_3$ as indicated in the first step, then PION@E6 were synthesized by means of phase transfer using the collected oleic acid coated IONs, DSPE-PEG 2000 and chlorin e6 as indicated in the second step (Figure 1).

The average hydrate particle size and zeta potential of PION@E6 were found to be 37.86±12.90 nm and –23.8 mV (Figure 2A,B), respectively, and uniformly distributed

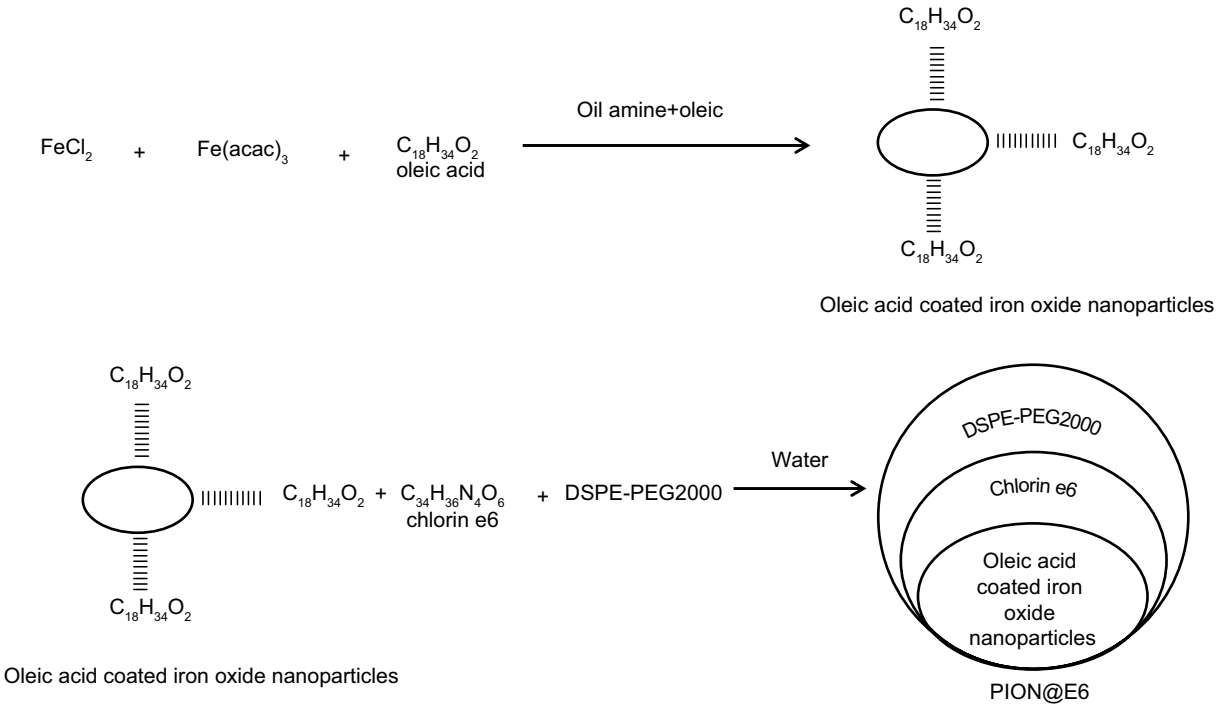

Figure 1 Two steps process for synthesizing the PION@E6.
Abbreviations: DSPE-PEG200, 2-distearoyl-sn-glycero-3-phosphoethanolamine-N-[methoxy(polyethylene glycol)-2000]; PION@E6, PEGylated iron oxide nanoparticles.

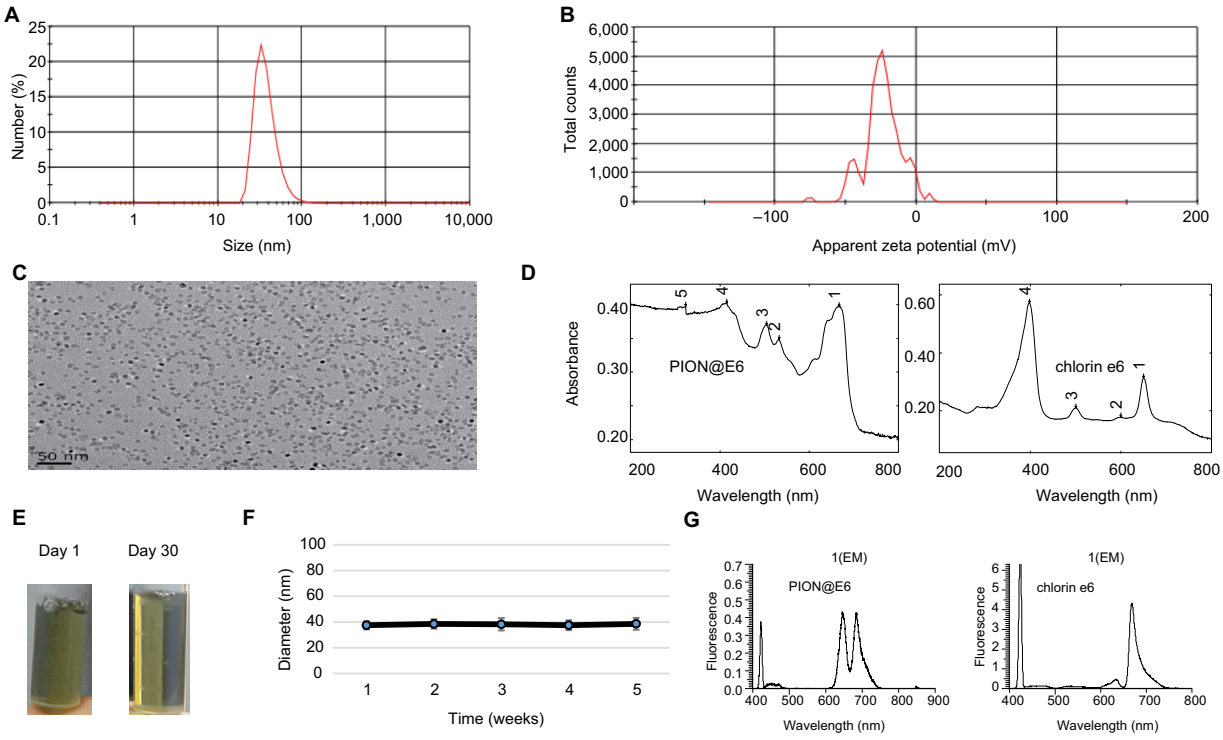

Figure 2 Identification and characterization of PION@E6.
Notes: (**A**) Hydrate particle size of PION@E6. (**B**) Zeta potential of PION@E6. (**C**) Representative photo of PION@E6 under TEM (Bar =50 μm in the field). (**D**) Absorption spectra of both PION@E6 and free E6. (**E**) Representative photos of aqueous solutions of PION@E6 taken at the first day and the thirtieth day. (**F**) Colloid stability test of PION@E6 dissolved in deionized water. (**G**) Fluorescence spectra of PION@E6 and chlorin e6.
Abbreviations: PION@E6, PEGylated iron oxide nanoparticles; TEM, transmission electron microscopy.

nanoparticles with an average diameter of 10 nm were observed under TEM (Figure 2C). Notably, chlorin e6 incorporated onto the PION@E6 was demonstrated by ultraviolet and visible absorption spectrophotometry (Figure 2D). Even though PION@E6 was suspended in deionized water for 30 days, no precipitation was observed (Figure 2E). Colloid stability test further demonstrated that no significant aggregation of PION@E6 was detected in the deionized water after 5 weeks (Figure 2F). Of note, the fluorescence excitation of PION@E6 was greatly shifted to the longer wavelength in the fluorescence excitation experiment (Figure 2G).

Cellular uptake of PION@E6

After incubation with 50 μg/mL PION@E6 for 2 hours, uptake of PION@E6 by U251 cells was demonstrated by the positive cytoplasmic Prussian blue granules (Figure 3B) as compared with bright image (Figure 3A), suggesting that PION@E6 could be successfully taken up by U251 cells. Notably, when incubated with various doses of PION@E6 for 24 hours, the relative cell viability of U251 cells showed no distinct difference even at a dose as high as 200 μg/mL; whereas at the time point of 72 hours, high dose (100 and 200 μg/mL) of PION@E6 showed significant impairment on the cell viability of U251 cells as compared with the control (Figure 4).

Migration and invasion of U251 cells treated with PION@E6 in the presence or absence of autophagy inhibitor 3-MA

As shown in Figure 5, after incubation with 200 μg/mL PION@E6 for 24 hours, the number of migratory U251 cells across transwell membrane decreased significantly as compared with that without PION@E6 treatment. When U251 cells were pretreated with 5 mm 3-MA and then treated with 200 μg/mL PION@E6 for an additional 24 hours, the number of migratory U251 cells increased significantly, as compared with that in the absence of 3-MA (Figure 5A and B), indicating the ability of PION@E6 to suppress the migration of U251 cells could be counteracted by pretreatment with 5 mm 3-MA.

As shown in Figure 6, after incubation with 200 μg/mL PION@E6 for 24 hours, the number of invasive U251 cells through Matrigel decreased significantly as compared with that without PION@E6 treatment. When U251 cells were pretreated with 5 mm 3-MA and then treated with 200 μg/mL PION@E6 for an additional 24 hours, the number of invasive U251 cells increased significantly, compared with

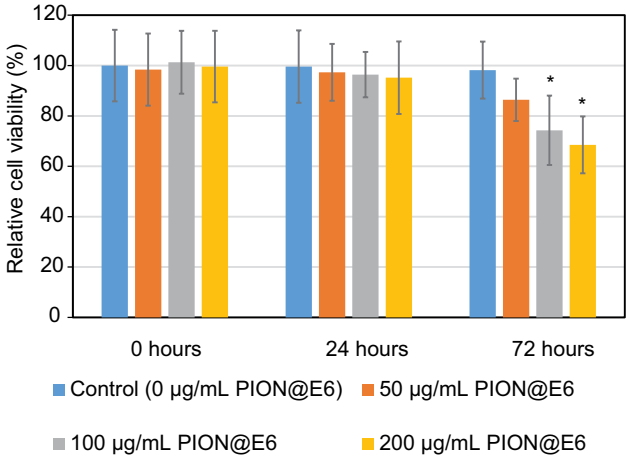

Figure 4 Cell viability of U251 cells incubated with various concentration of PION@E6 for 24 hours.
Notes: Error bars were based on SD of 4 samples. *P<0.05, compared with control group.
Abbreviation: PION@E6, PEGylated iron oxide nanoparticles.

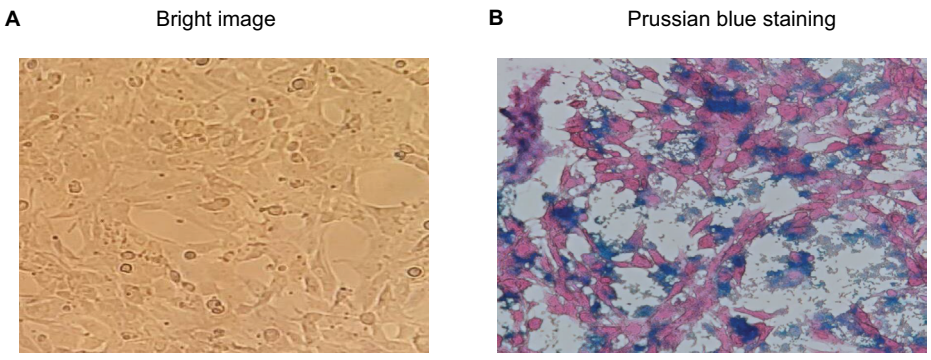

Figure 3 Uptake of PION@E6 by U251 cells incubated with 50 μg/mL of PION@E6 for 2 hours.
Notes: (**A**) Bright imaging of U251 cells (magnification ×200); (**B**) Representative image of U251 cells stained with Prussian blue (magnification ×200).
Abbreviation: PION@E6, PEGylated iron oxide nanoparticles.

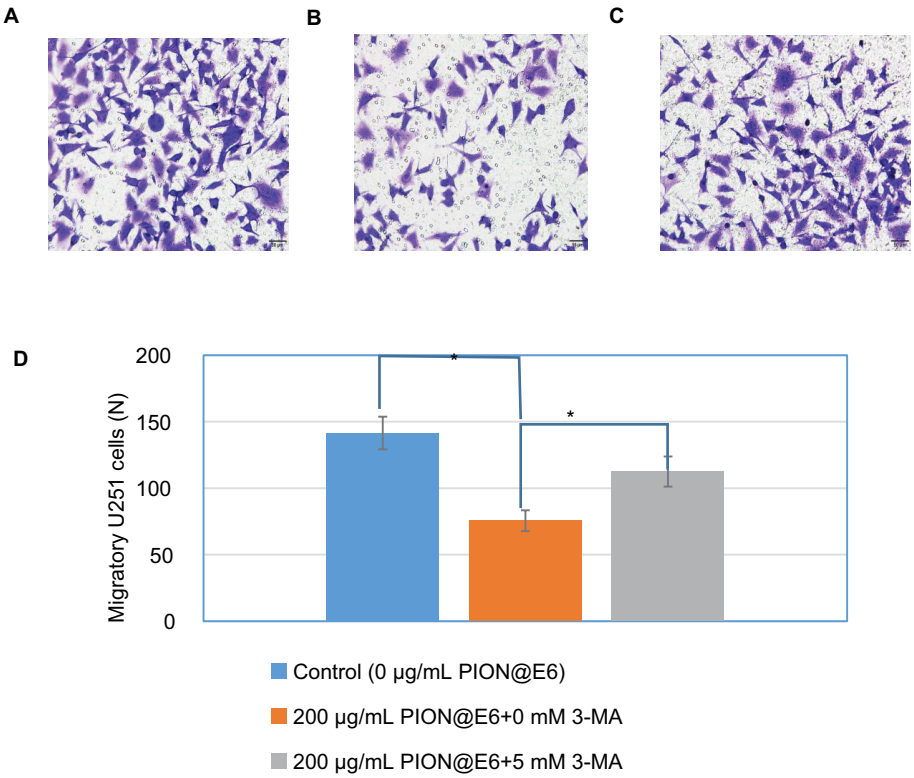

Figure 5 Migration of U251 cells incubated with 200 μg/mL PION@E6 in the presence or absence of autophagy inhibitor 3-MA.
Notes: (**A**) Representative image of migratory U251 cells (×200) by crystal violet staining after incubation with 0 μg/mL PION@E6 for 24 hours in the absence of 3-MA. (**B**) Representative image of migratory U251 cells (×200) by crystal violet staining after incubation with 200 μg/mL PION@E6 for 24 hours in the absence of 3-MA. (**C**) Representative image of migratory U251 cells (×200) by crystal violet staining after incubation with 200 μg/mL PION@E6 for 24 hours in the presence of 3-MA. (**D**) Number of migratory U251 cells per field of microscopy view. Error bars were as based on SD of 3 replicates. *P<0.05, statistically significant.
Abbreviations: 3-MA, 3-methyladenine; PION@E6, PEGylated iron oxide nanoparticles.

those in the absence of 3-MA (Figure 6), indicating the ability of PION@E6 to suppress the invasion of U251 cells could be counteracted by pretreatment with 5 mm 3-MA. Furthermore, Figure 7 showed that the inhibition of cell invasion increased with the increasing concentration of PION@E6 (Figure 7), suggesting that this inhibitory effect of PION@E6 on the invasion of U251 cells is in a dose-dependent manner.

Expression of autophagy-related proteins in U251 cells

Relative expression of beclin-1 protein in U251 cells increased with the increasing concentration of PION@E6 (P<0.05, Figure 8A and C). Similarly, the expression level of LC3II protein relative to LC3I in U251 cells increased with the increasing concentration of PION@E6 (P<0.05, Figure 8B,D), whereas that of P62 protein decreased with increasing dose of PION@E6(P<0.05, Figure 8A and C). These results suggested that PION@E6 could promote the autophagy in U251 cells.

Intracellular ROS generation promoted by PION@E6

As compared with control group, a remarkable fluorescent enhancement was detected by Spectra Max fluorescence microplate reader (Molecular Devices LLC) after treatment with PION@E6 for 12 hours, which corresponded to the increased level of ROS in the U251 cells. Notably, the fluorescence values in U251 cells increased with the increasing concentration of PION@E6 (P<0.05), indicating a PION@E6 dose-dependent intracellular ROS generation (Figure 9).

Discussion

Polyethylene glycol (PEG) is a polymer of ethylene oxide units that was adopted to maintain circulation stability in the blood. Previous study reported that nanoparticles possessing PEG chains on their surface have been described as blood persistent drug delivery system with potential applications for intravenous drug administration.[14] As expected, PEGylated PION@E6 in our present study have been found

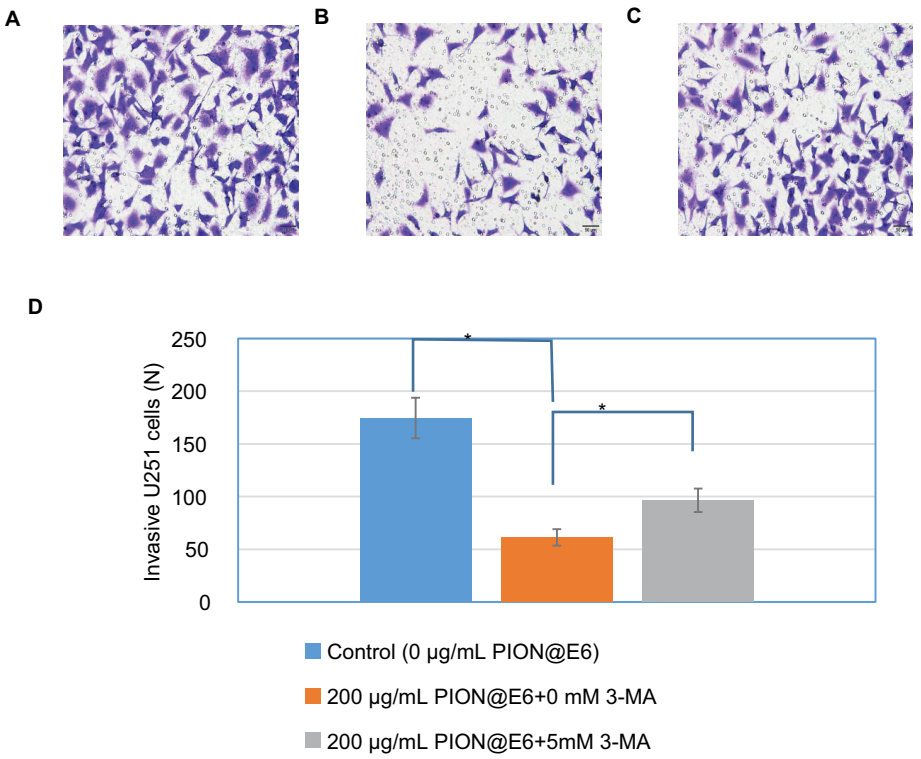

Figure 6 Invasion of U251 cells incubated with 200 μg/mL PION@E6 in the presence or absence of autophagy inhibitor 3-MA.
Notes: (**A**) Representative image of invasive U251 cells (×200) by crystal violet staining after incubation with 0 μg/mL PION@E6 for 24 hours in the absence of 3-MA. (**B**) Representative image of invasive U251 cells (×200) by crystal violet staining after incubation with 200 μg/mL PION@E6 for 24 hours in the absence of 3-MA. (**C**) Representative image of invasive U251 cells (×200) by crystal violet staining after incubation with 200 μg/mL PION@E6 for 24 hours in the presence of 3-MA. (**D**) Number of invasive U251 cells per field of microscopy view. Error bars were as based on SD of 3 replicates. *P<0.05, statistically significant.
Abbreviations: 3-MA, 3-methyladenine; PION@E6, PEGylated iron oxide nanoparticles.

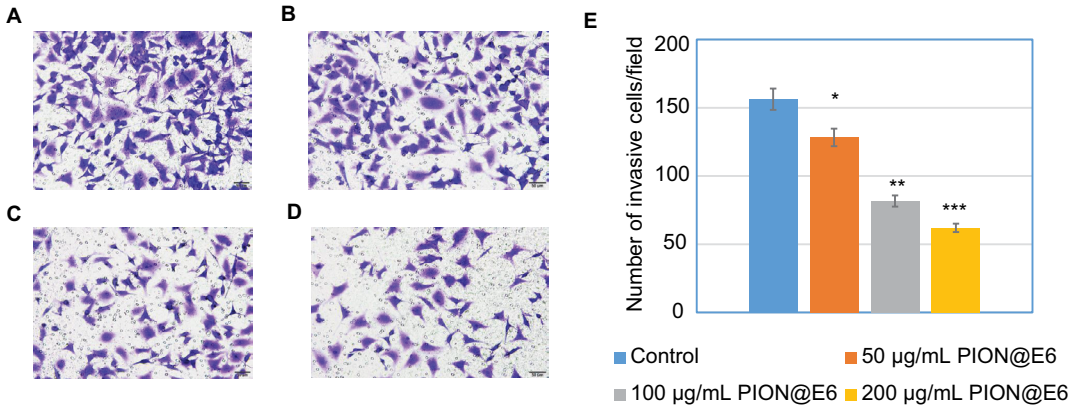

Figure 7 Invasion of U251 cells incubated with different concentrations of PION@E6 for 24 hours.
Notes: The representative images of invasive U251 cells (×200) treated by different concentrations of PION@E6 by crystal violet staining (**A**–**D**). (**A**) Control. (**B**) 50 μg/mL PION@E6. (**C**) 100 μg/mL PION@E6. (**D**) 200 μg/mL PION@E6. (**E**) Number of invasive U251 cells per field of microscopy view. Each group consists of 3 replicates. Error bars were based on SD of 3 replicates. *P<0.05, compared with control group. **P<0.05, compared with those treated with 50 μg/mL PIONs@E6. ***P<0.05, compared with those treated with 100 μg/mL PION@E6.
Abbreviation: PION@E6, PEGylated iron oxide nanoparticles.

to possess brilliant solubility and stability, as demonstrated by the fact that no significant aggregation of nanoparticles were observed after being well-dispersed and dissolved in the aqueous solution for a long time. In addition, the PEG functionalization and incorporation of chlorin e6 onto nanoparticles were directly confirmed by the absorption spectra and size distribution of PION@E6. All these facts mentioned above are expected to bring an in vitro stability and

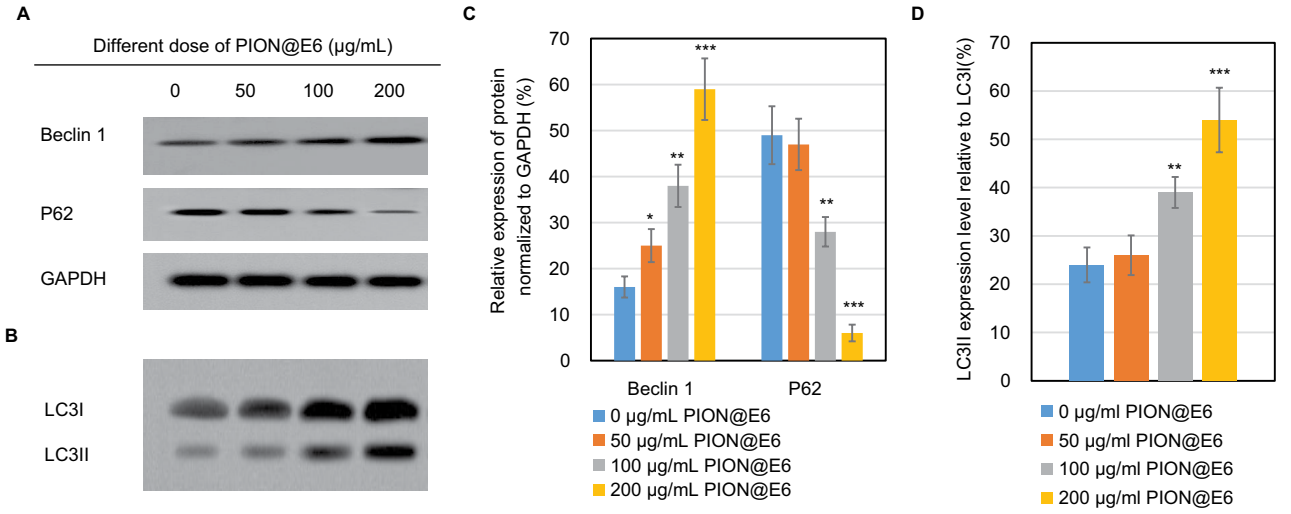

Figure 8 Expression of key regulator of autophagy-related proteins in U251 cells incubated with different concentrations of PIONs for 24 hours.
Notes: (**A**) Expression of beclin-1 and P62 proteins in U251 cells determined by Western blotting. (**B**) Expression of LC3 protein in U251 cells by Western blotting. (**C**) Relative expression of beclin-1 and P62 proteins normalized to GAPDH in U251 cells. (**D**) Relative expression of LC3II relative to LC3I protein in U251 cells. Error bars were based on SD of 3 replicates. **P*<0.05, compared with control group. ***P*<0.05, compared with those incubated with 50 μg/mL PION@E6. ****P*<0.05, compared with those incubated with 100 μg/mL PION@E6.
Abbreviations: GAPDH, glyceraldehyde 3-phosphate dehydrogenase; PION@E6, PEGylated iron oxide nanoparticles.

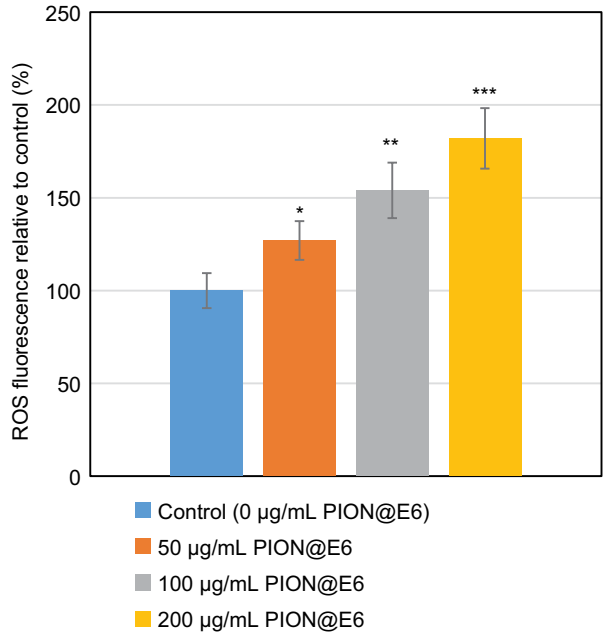

Figure 9 Relative intracellular ROS in the U251 cells when incubation with different concentrations of PIONs@E6 for 12 hours.
Notes: Each group consists of 8 samples. Error bars were based on SD of 8 samples. **P*<0.05, compared with control group. ***P*<0.05, compared with those incubated with 50 μg/mL PION@E6. ****P*<0.05, compared with those incubated with 100 μg/mL PION@E6.
Abbreviation: PION@E6, PEGylated iron oxide nanoparticles.

a long blood circulation time of PION@E6, and a consequent tumor homing ability of PION@E6 relying on the "enhanced permeability and retention" effect of solid tumors.[15,16] Additionally, the spectral peak of E6 with an obvious red-shift from 660 nm to 695 nm was observed after being loaded on PEGylated IONs in the present study. Incubation of U251 cells with PION@E6 for 2 hours is sufficient for its cellular uptake (Figure 3), which was directly demonstrated by the positive cytoplasmic Prussian blue granules. Moreover, the long treatment (72 hours) with PION@E6 showed significant impairment on the cell viability of U251 cells.

As we know, the notable features of GBM cells are invasion into surrounding tissues.[17] Cell migration and invasion are multistep complex processes, requiring coordinated activities of cytoskeleton, membrane and adhesion systems. It has recently been demonstrated that invasiveness is considered as a major determinant for malignant behavior in human gliomas and U251 cells represent a highly invasive tumor.[18]

As shown in Figures 5 and 6, after incubation with 200 μg/mL PION@E6 for 24 hours, the migration and invasion of U251 cells were significantly inhibited compared with that without PION@E6 treatment. Furthermore, the inhibition of cell invasion increased with the increasing concentration of PION@E6 (Figure 7), suggesting that this inhibitory effect of PION@E6 on the invasion of U251 cells is in a dose-dependent manner.

3-MA, a cell-permeable autophagic sequestration blocker, is commonly used as autophagy inhibitor by blocking the formation of autophagosomes.[19,20] When U251 cells were pretreated with 5 mm 3-MA and then treated with 200 μg/mL PION@E6 for an additional 24 hours, the migration and

invasion of U251 cells increased significantly, compared with that in the absence of 3-MA (Figure 5A and B), indicating the ability of PION@E6 to suppress the migration/invasion of U251 cells could be counteracted by autophagy inhibitor 3-MA.

Autophagy is an intracellular degradation system in which proteins and organelles are sequestered, degraded and recycled.[21] It has been demonstrated that microtubule-associated protein 1 light chain 3 (LC3), p62, and beclin-1 are central autophagy-related proteins involved in the autophagy flux.[22] LC3 II (isoform II of light chain) was inserted in the inner and outer layers of the autophagosomal vesicles to format the hallmark of autophagosome. Notably, the LC3-II to LC3-I ratio was reported to be proportional to the number of autophagic vacuoles.[23] Our present results demonstrated that the expression level of LC3II protein relative to LC3I in U251 cells increased with the increasing PION@E6 concentration. Additionally, p62 is a selective autophagy substrate, continuously degraded by autophagy;[22] *beclin-1*, a tumor suppressor gene, is an autophagy-specific protein that regulates autophagosome formation.[24–26] The present results of Western blotting demonstrated a significant higher expression of *beclin-1* and a lower expression of p62 autophagic proteins in U251 cells in a dose-dependent manner of PION@E6. These facts suggest that PION@E6 could promote the autophagy in U251 cells.

More recently, other reports found that promotion of autophagy could impair the invasion of KRAS-transformed cells, while interrupting autophagy could counteract the inhibitory effect on the invasion of transformed cells, which was further demonstrated in mice bearing transformed cells-derived tumor xenograft by inducing autophagy.[5,6] However, other reports demonstrated that cancer cells proliferation is related to autophagy elevation, possibly due to the increased metabolic and biosynthetic demands imposed by deregulated profiferation.[27–29]

In the setting of PION@E6 treatment in our present study, it is tempting to speculate that most of the autophagy, though elevated by PION@E6, was turned to sequester PION@E6 for lysosome degradation, rather than to support the metabolic and biosynthetic demands imposed by cancer cells, thus leading to the limitation of cell viability and invasiveness. Moreover, it was previously reported that lysosomal iron liberation from IONs and iron-catalyzed ROS generation in the lysosomal degradation pathway is responsible for the ION-induced toxicity of microglia.[30] Inhibition of autophagy by 3-MA in our study may reduce the autophagy related lysosomal degradation of IONs and its related iron liberation and excess ROS production, finally counteracting the invasiveness inhibitory effect of PION@E6 on glioma cells.

Collectively, it is reasonable to suggest that PION@E6 may be able to induce a strong elevation of autophagy, which may be related to the impairment of the cell viability and invasiveness of U251 cells. However, this invasion inhibition effect of PION@e6 should be further verified in vivo in mice bearing GBM. Meanwhile, whether PION@E6 could cross the blood brain barrier to access GBM should be elucidated in the future research.

Autophagy is increased in cells in face of metabolic stresses including growth factor withdrawal, nutrient deprivation, and hypoxia.[8] Hence, it has most likely evolved as a quality control mechanism to protect the cell against damage caused by toxic macromolecules such as ROS and its related radicals.[31] Previous studies reported that an increased level of ROS triggered the cell to respond by inducing autophagy for cytoprotection owing to their damaging effects on cellular proteins, lipids and DNA.[32] Using U251 cells from human GBM, our experiment demonstrated that the ROS level in U251 cells increased with the increasing concentration of PION@E6 ($P<0.05$), indicating PIONs argument intracellular ROS generation in a dose-dependent manner. These results suggested that autophagy may be associated with the intracellular levels of ROS and PION@E6 may promote autophagy through ROS generation. However, this fact needs to be further demonstrated in future experiments by depletion of ROS.

Conclusion

Taken together, invasiveness of human GBM cells involves the PION@E6 mediated autophagy process, which may be related to the generation of intracellular ROS induced by PION@E6. The further research on the possible pathway in the PION@E6 mediated autophagy process may be helpful for deep understanding of the mechanism for suppressing the invasiveness of GBM cells.

Acknowledgments

The authors thank Professor Guohua Xia for his kind help in the manuscript processing. This work was supported by Guangxi Nature and Science Fund (project nos. 2017GXNSFAA198112 and 2015GXNSFBA139135).

Disclosure

The authors report no conflicts of interest in this work.

References

1. Lu B, Zhou Y, Su Z, Ding P. Effect of CCL2 siRNA on the cell migration and adhesion in human glioma cell lines U251 and U373. *Int J Clin Exp Pathol*. 2017;10(1):771–780.
2. Wu M, Miska J, Xiao T, et al. Race influences survival in glioblastoma patients with KPS ≥ 80 and associates with genetic markers of retinoic acid metabolism. *J Neurooncol*. Epub 2019 Jan 31.
3. Tchaicha JH, Reyes SB, Shin J, Hossain MG, Lang FF, McCarty JH. Glioblastoma angiogenesis and tumor cell invasiveness are differentially regulated by 8 integrin. *Cancer Res*. 2011;71(20):6371–6381.
4. Chen G, Roy I, Yang C, Prasad PN. Nanochemistry and nanomedicine for nanoparticle-based diagnostics and therapy. *Chem. Rev*. 2016;116(5):2826–2885.
5. Luo X, Cheng W, Wang S, Chen Z, Tan J. Autophagy suppresses invasiveness of endometrial cells through reduction of fascin-1. *Biomed Res Int*. 2018;2018:1–9.
6. Liu J, Zheng L, Ma L, et al. Oleanolic acid inhibits proliferation and invasiveness of Kras-transformed cells via autophagy. *J Nutr Biochem*. 2014;25(11):1154–1160.
7. Zhang P, Ren Z, Chen Z, et al. Iron oxide nanoparticles as nanocarriers to improve chlorin e6 based sonosensitivity in sonodynamic therapy. *Drug Design Development and Therapy*. 2018;12:4207–4216.
8. Poillet-Perez L, Despouy G, Delage-Mourroux R, Boyer-Guittaut M. Interplay between ROS and autophagy in cancer cells, from tumor initiation to cancer therapy. *Redox Biology*. 2015;4:184–192.
9. Efeyan A, Comb WC, Sabatini DM. Nutrient-sensing mechanisms and pathways. *Nature*. 2015;517(7534):302–310.
10. Guo JY, Autophagy WE. Metabolism, and cancer. *Cold Spring Harb Symp Quant Biol*. 2016;81:73–78.
11. Mizushima N, Levine B, Cuervo AM, Klionsky DJ. Autophagy fights disease through cellular self-digestion. *Nature*. 2008;451(7182):1069–1075.
12. Indelicato M, Pucci B, Schito L, et al. Role of hypoxia and autophagy in MDA-MB-231 invasiveness. *J Cell Physiol*. 2010;223:359–368.
13. Degenhardt K, Mathew R, Beaudoin B, et al. Autophagy promotes tumor cell survival and restricts necrosis, inflammation, and tumorigenesis. *Cancer Cell*. 2006;10(1):51–64.
14. Gref R, Lück M, Quellec P, et al. 'Stealth' corona-core nanoparticles surface modified by polyethylene glycol (PEG): influences of the corona (PEG chain length and surface density) and of the core composition on phagocytic uptake and plasma protein adsorption. *Colloids Surf B Biointerfaces*. 2000;18(3-4):301–313.
15. Thambi T, You DG, Han HS, et al. Bioreducible carboxymethyl dextran nanoparticles for tumor-targeted drug delivery. *Adv. Healthc Mater.* 2014;3(11):1829–1838.
16. Thambi T, Deepagan VG, Yoon HY, et al. Hypoxia-responsive polymeric nanoparticles for tumor-targeted drug delivery. *Biomaterials*. 2014;35(5):1735–1743.
17. Liotta LA, Nageswara Rao C, Wewer UM. Biochemical interactions of tumor cells with the basement membrane. *Ann Rev Biochem*. 1986;55(1):1037–1057.
18. Mecca C, Giambanco I, Bruscoli S, et al. PP242 counteracts glioblastoma cell proliferation, migration, invasiveness and stemness properties by inhibiting mTORC2/Akt. *Front. Cell. Neurosci*. 2018; 12:99.
19. Su Y, Lu J, Chen X, et al. Long non-coding RNA HOTTIP affects renal cell carcinoma progression by regulating autophagy via the PI3K/Akt/Atg13 signaling pathway. *J Cancer Res Clin Oncol*. 2018;2014.
20. Cao Y, Luo Y, Zou J, et al. Autophagy and its role in gastric cancer. *Clin Chim Acta*. 2019;489:10–20.
21. Baehrecke EH. Autophagy: dual roles in life and death? *Nat Rev Mol Cell Biol*. 2005;6(6):505–510.
22. Schläfli AM, Berezowska S, Adams O, Langer R, Tschan MP. Reliable LC3 and p62 autophagy marker detection in formalin fixed paraffin embedded human tissue by immunohistochemistry. *Eur J Histochem*. 2015;59(2):2481.
23. Klionsky DJ, Abdalla FC, Abeliovich H, et al. Guidelines for the use and interpretation of assays for monitoring autophagy. *Autophagy*. 2012;8(4):445–544.
24. Pattingre S, Espert L, Biard-Piechaczyk M, Codogno P. Regulation of macroautophagy by mTOR and Beclin 1 complexes. *Biochimie*. 2008;90(2):313–323.
25. Kessel D, Reiners JJ. Apoptosis and autophagy after mitochondrial or endoplasmic reticulum photodamage. *Photochem Photobiol*. 2007;83(5):1024–1028.
26. Tang X, Mo C, Wang Y, Wei D, Xiao H. Anti-tumour strategies aiming to target tumour-associated macrophages. *Immunology*. 2013;138(2):93–104.
27. Yang S, Wang X, Contino G, Li Y, Haigis M. Pancreatic cancers require autophagy for tumor growth. *Genes Dev*. 2011;25(7):717–729.
28. Lock R, Kenific CM, Leidal AM, Salas E, Debnath J. Autophagy-dependent production of secreted factors facilitates oncogenic RAS-driven invasion. *Cancer Discov*. 2014;4(4):466–479.
29. Mowers EE, Sharifi MN, Macleod KF. Autophagy in cancer metastasis. *Oncogene*. 2017;36(12):1619–1630.
30. Petters C, Thiel K, Dringen R. Lysosomal iron liberation is responsible for the vulnerability of brain microglial cells to iron oxide nanoparticles: comparison with neurons and astrocytes. *Nanotoxicology*. 2016;10(3):332–342.
31. Chiarugi P, Giannoni E. Anoikis: a necessary death program for anchorage-dependent cells. *Biochem Pharmacol*. 2008;76(11):1352–1364.
32. Johansson I, Monsen VT, Pettersen K, et al. The marine n-3 PUFA DHA evokes cytoprotection against oxidative stress and protein misfolding by inducing autophagy and NFE2l2 in human retinal pigment epithelial cells. *Autophagy*. 2015;11(9):1636–1651.